Polarization controlled coupling and shaping of surface plasmon polaritons by nanoantenna arrays

Ori Avayu,* Itai Epstein, Elad Eizner, and Tal Ellenbogen

Department of Physical Electronics, Fleischman Faculty of Engineering, Tel Aviv University, Tel Aviv 69978, Israel
**Corresponding author: oria@post.tau.ac.il*

Received December 16, 2014; revised March 4, 2015; accepted March 5, 2015;
posted March 6, 2015 (Doc. ID 229300); published March 27, 2015

We demonstrate experimentally the use of ordered arrays of nanoantennas for polarization controlled plasmonic beam shaping and excitation. Rod- and cross-shaped nanoantennas are used as local point-like sources of surface plasmon polaritons, and the desired phase of the generated plasmonic beam is set directly through their spatial arrangement. The polarization selectivity of the optical nanoantennas allows us to further control the excitation, enabling the realization of a variety of complex and functional plasmonic beam shaping elements. We demonstrate this concept by generating plasmonic self-accelerating beams, plasmonic bottle beams, and switchable dual-focii plasmonic lenses. The freedom in the design and arrangement of these nanoantennas enables us to specifically tailor and control the shapes, wavelengths, and coupling efficiencies of complex plasmonic beams.

OCIS codes: (240.5440) Polarization-selective devices; (050.6624) Subwavelength structures; (240.6680) Surface plasmons; (160.4236) Nanomaterials; (220.4000) Microstructure fabrication.
http://dx.doi.org/10.1364/OL.40.001520

Surface plasmon polaritons (SPPs) are surface electromagnetic waves that propagate along an interface between a metal and a dielectric [1]. The high spatial confinement of these beams holds promise for a variety of optoelectronics and nanophotonics applications [2–5], including biochemical sensing, spectroscopy and trapping [6,7], plasmon wave guiding for telecommunication [8], and sub-wavelength interferometry [9]. In light of these exciting possibilities, the ability to manipulate and control the shape of the SPP wavefront received much attention recently, and the generation of unique nondiffracting Airy, Mathieu, Weber, and Bessel plasmonic beams [10–12] was demonstrated.

It is well known, however, that launching a plasmonic beam presents a fundamental difficulty. For a given frequency, the wave-vector of the SPP, k_{spp}, is larger than its free-space counterpart. Therefore, to couple an SPP from free space, it is necessary to overcome this wave-vector mismatch. This is commonly achieved by using prism or grating couplers. Prisms are usually large and, thereby, cannot be used for compact devices. Gratings can be integrated and fabricated with excellent precision, and indeed metallic grating-based plasmonic holograms have been used to demonstrate plasmonic beam shaping [10,12–15]. However, the use of gratings also possess some limitations. First, the coupling efficiency depends on the number of periods of the grating and, for efficient coupling, the grating can extend over tens of microns. Second, gratings are polarization dependent in such a way that only the TM part of the illuminated beam couples to an SPP. Third, as discussed by Epstein and Arie [13,14], there is a fundamental limitation on the amount of transverse phase difference that can be realized by it, and this puts a limit on the spatial frequencies that can be generated. Therefore, to generate a well-defined phase profile for an SPP, the grating structure should be as short as possible, which drastically reduces the coupling efficiency.

Coupling light to surface plasmons in a localized manner addresses the issues mentioned above and, indeed, several techniques have been suggested, including near-field probe [16] and e-beam excitation [17]. These methods, however, require an external electronic feedback mechanism, which makes them expensive and inappropriate for many applications. An alternative approach to locally excite SPPs, and to compensate for the wave-vector mismatch is to use sub-wavelength metallic nanostructures which serve as scattering centers and couple light to SPPs [18,19]. These nanostructures can be engineered to have a resonant response at a desired wavelength and polarization, for which their scattering efficiency is highly increased. Because of their ability to convert far-field radiation to near-field currents, and vice-versa, they are sometimes treated as optical nanoantennas [20].

Recently, metallic nanoparticles and nanoantennas were suggested for different coupling schemes [21–25] and functional beam shaping [26]. In particular, arrays of nanoslits were proposed for interesting applications, including polarization-controlled directional SPP launching [27] and optical-spin manipulations [28,29]. These methods demonstrate the advantages of using nanoparticles and nanoantennas to manipulate light and SPPs with high efficiency (1%–3% [27], compared to previously estimated 0.35% for gratings [14]), and compact geometry. To increase the functionality of these SPP couplers and allow the generation of more complex plasmonic beam characteristics, new means of controlling the SPP wavefront are of great interest.

In this Letter, we present a general method for shaping plasmonic beams with chains of rod and cross-shaped nanoantennas. Specifically, we present the design criteria for generating arbitrarily self-accelerating SPP beams, demonstrate experimentally a number of illustrative examples and show that this method enables us to achieve almost twice as much higher acceleration rates, compared with those previously reported by using a standard grating mask [13]. We also show how the polarization selective coupling mechanism of the nanoantennas allows us to obtain intensity modulation of these

self-accelerating beams, and to create a dual focii lens element that switches intensity levels between two focal spots.

To analyze the scattering properties of nanoantennas we performed finite difference time domain simulations. Figure 1(a) shows simulation results of scattering from a silver nanoantenna which is placed above a silver film. The color scale shows the normal component of the electric field, and the arrow indicates the input polarization. It can be seen that the nanoantenna excites SPPs with a point dipole field distribution [30]. The total power of light converted to a propagating SPP is a function of the dot product of the light field and the principal axis of the nanoantenna. Consequently, we define the differential coupling strength ratio as the ratio between the maximal and minimal coupling strengths obtained for light polarized along, or perpendicular, to the principal axis of the nanoantenna, respectively. We use rod shaped nanoantennas with dimensions $l = 600$ nm, $w = 100$ nm, and $h = 130$ nm where l, w, and h are the length, width, and height of the nanoantenna, respectively. The nanoantennas were designed to have an optimal coupling to SPPs at a free-space wavelength of $\lambda = 1.064$ μm ($\lambda_{spp} = 1.054$ μm), and a coupling strength ratio of more than one order of magnitude between polarizations along the long or short axis of the nanoantenna.

To shape the surface plasmon wavefront, we consider a chain of nanoantennas, with a spacing smaller than the wavelength. Each nanoantenna then acts as an SPP point-like source with relative phase that depends on $\Delta z/\lambda_{spp}$, where z is the propagation direction. In the simplest case, when the nanoantennas are ordered along a straight line ($z = 0$ plane), the SPP field distribution will be that of a plane wave propagating away from both sides of the chain ($\pm z$ directions) with equal intensity [27]. If we now arrange the nanoantennas in a more complex configuration, local phase changes can be controlled and unique SPP beam shapes can be obtained.

The fabrication of the nanoantennas was done by evaporating 200 nm of silver on a glass substrate, followed by e-beam lithography of the nanoantennas pattern on polymethyl methacrylate (PMMA). A 130 nm silver layer was evaporated above the PMMA, followed by a liftoff process. The final device consisted of 130 nm thick silver nanoantennas, on top of a 200 nm layer of silver. The inter-spacing between the nanoantennas was kept sub-wavelength with a center-to-center distance of 600 nm to avoid near-field interactions between adjacent neighboring nanoantennas which can reduce the coupling. The experimental setup, illustrated in Fig. 1(b), was composed of light from a fiber-coupled diode pumped laser ($\lambda = 1.064$ μm), focused on the sample by a cylindrical lens and a microscope objective lens. The Nanonics MultiView 2000 NSOM system was used to measure the plasmonic light intensity.

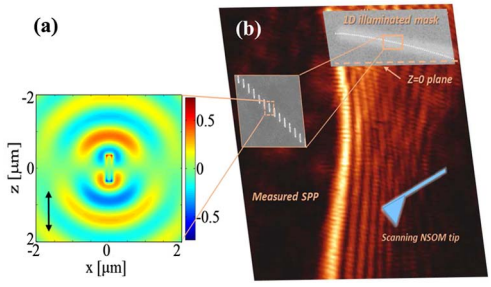

Fig. 1. (a) Simulation of the normal to surface component of the emanating SPP field from a single nanoantenna in resonance when the incoming field is polarized along its principal axis (arrow indicating the input polarization). (b) Illustration of the experimental setup.

First, we examine the case of plasmonic self-accelerating beams traveling along a convex arbitrary trajectory $y = c(z)$. It was previously shown that self-accelerating beams can be constructed by multiple geometrical rays that are tangent to the curve of the beam [31,32]. To generate these rays at angles $\theta(y)$, an initial known transverse phase $\phi(y)$ in the plane $z = 0$ should be excited, and can be obtained by numerically solving [31] $\frac{d\phi(y)}{dy} = \frac{kc'(z)}{\sqrt{1+(c'(z))^2}}$, where $c' = dc/dz$. This was previously done by encoding the phase, $\phi(y)$, into a plasmonic hologram based on a binary modulated grating [13,14]. In our case, $\phi(y)$ is set directly by spatially arranging the nanoantennas along the curve $\phi(y)$. This results in an ordered chain of nanoantennas, as illustrated in Fig. 1(b), reducing considerably the previous several microns size hologram to nanometric size. Therefore, the collective phase contribution of propagating SPPs from all the nanoantennas at the $z = 0$ plane generates the geometrical rays constructing the self-accelerating surface plasmon.

Figure 2 shows experimental measurements from antenna based SPP couplers generating self-accelerating

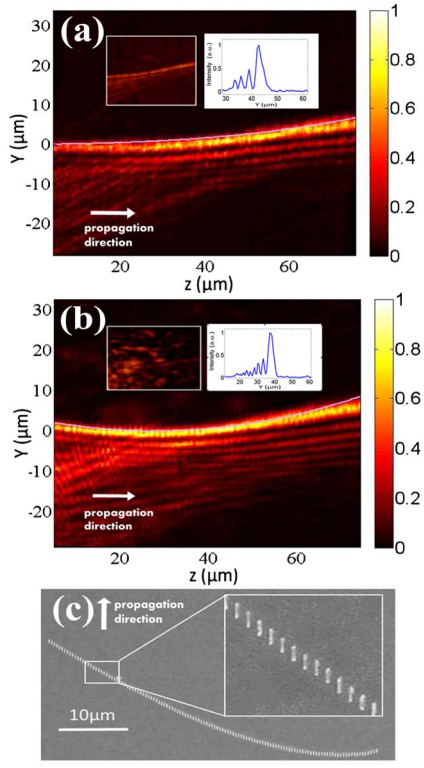

Fig. 2. Experimental results of caustic beams with (a) cubic trajectory and (b) parabolic trajectory (scale bar normalized to 1). (c) SEM micrograph image of the fabricated devices.

plasmonic beams with beam trajectories of $y = az^3$ [Fig. 2(a)] and $y = az^2$ [Fig. 2(b)], where a is the acceleration strength parameter. The purple line plotted along the main lobe of the beam shows the designed analytical trajectory, $c(z)$, of each beam, indicating a good agreement between the measured SPP trajectory and the target trajectory. The transverse cross section of the two beams reveals the Airy like profile of the measured SPP (see inset), as expected from theory [32]. In this case, the nanoantennas case are oriented along the z direction, and the incident light is polarized along this direction. To measure the coupling strength ratio, we performed also scans when the incident light polarization was perpendicular to the nanoantenna principal axis. The coupling strength ratio was then calculated as the ratio of the intensities of the main lobe of the beam at the two incident polarizations. The insets of Figs. 2(a) and 2(b) show the measured SPP when the input polarization was along the short axis of the nanoantenna (scaling is identical for the main image and the inset). The coupling strength ratios that were measured for the cubic trajectory SPP and parabolic trajectory SPP were 3 and 8, respectively. We attribute the difference between the ratios in the two samples to fabrication imperfections and to differences in the alignment of the illumination in the two measurements.

As an example of the advantage of this coupling method over coupling with a grating, we chose acceleration parameter a in the case of the parabolic beam [Fig. 2(b)] to be 4×10^{-3} μm^{-1} compared to the maximal value of 2.4×10^{-3} μm^{-1}, which has previously been demonstrated [13]. These acceleration strength parameters cannot be targeted using grating coupling because of limitations of the grating coupling configuration. The flexibility of our method, which does not limit the obtained spatial frequencies, can be used to generate arbitrary relative phase.

Using this proposed method, we can realize more complex mask designs. As an example, we show the generation of a bottle beam, created by the intersection of two counter-accelerating beams. Bottle beams have been studied extensively, and their creation was already realized using different methods in both free space and plasmonics [14,33]. Figure 3 shows the result of a nanoantenna based bottle beam composed of two parabolic caustic curves. The initial phase at the $z = 0$ plane is now divided into $\phi^+(y)$ and $\phi^-(y)$, corresponding to the desired phase in the positive and negative y values, as seen in Fig. 3(a). The intensity switching capability of our design is specifically interesting for a variety of applications using bottle beams, such as particle trapping.

Finally, we use the polarization selectivity of the nanoantennas to demonstrate switchable a dual focii plasmonic lens. The dual focii lens was designed to launch and focus an SPP at two focal points, 80 and 60 μm in the z direction [Figs. 4(a) and 4(b)]. This lens consists of two chains of nanoantennas, where the nanoantennas in one chain are oriented along the x direction, and the nanoantennas in the second chain are oriented along the y direction. The intersection of the chains consists of cross-shaped nanoantennas. When we illuminate the device with x polarized light, one chain is on resonance, while the second chain generates an SPP with minimal intensity, corresponding to the calculated coupling strength ratio. We can, therefore, dynamically switch intensities between focal planes by changing the input polarization, or obtain equal intensity dual focii for an input polarization of 45°. The intensity switching capability of our device was measured by calculating the ratio of the maximum to minimum intensity at the focal point of each chain by switching the input polarization from x to y, and was found to be greater than 2. The SPP waves generating the two closely spaced focii interfere, because of this coupling ratio. We performed beam propagation simulations, calculated for the obtained coupling strength ratio [Figs. 4(c) and 4(d)] that demonstrate this behavior. The interference can be reduced, therefore, by selecting, for example, two focal spots farther apart, or in opposite z directions. In addition, we attribute the asymmetry of the device to our illumination scheme, since the two chains of nanoantennas have different curvatures and, therefore, have a slightly different response to the excitation beam.

In conclusion, we demonstrated experimentally the excitation and shaping of plasmonic beams using chains of nanoantennas. The design principles suggested in this

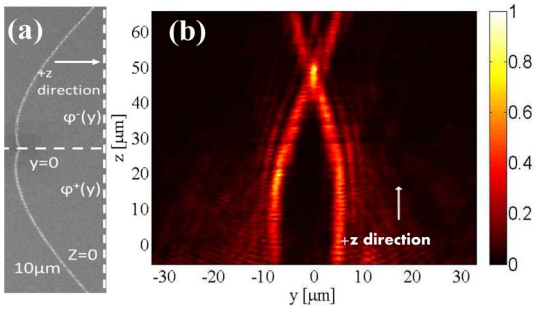

Fig. 3. (a) SEM micrograph image of the bottle beam device. Vertical dashed lines show the $z = 0$ plane and horizontal dashed lines divide the image into the $\pm y$ directions. (b) Measurement of the emanating SPP bottle beam.

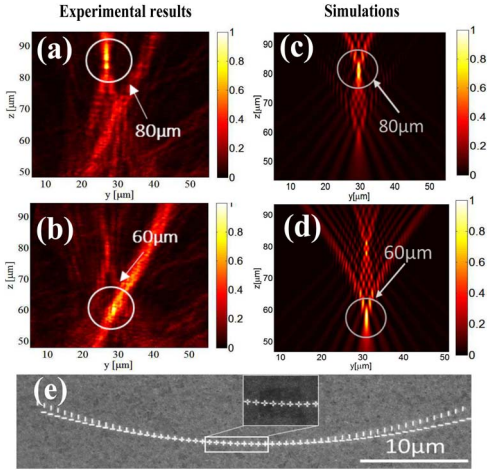

Fig. 4. (a) and (b) NSOM measurement of polarization controlled dual focii SPP lens, illuminated with (a) x and (b) y polarized light. (c) and (d) Simulation results of the dual focii lens. (e) SEM of the dual lens device.

Letter offer a general platform for exploring multi-functional compact plasmonic devices, using the polarization and wavelength selectivity of the nanoantenna SPP coupling mechanism. The point-like source excitation of SPPs by the nanoantennas enable us to generate arbitrary relative phases. The polarization response, described by the coupling strength ratio parameter, allows us to control the intensity of the generated SPP. We note that amplitude modulations can also be introduced by changing the length or orientation of the nanoantennas and, therefore, full control of both amplitude and phase can be achieved. In addition, the coupling efficiency could be increased easily by introducing correctly spaced multiple chains. We believe that the variety of shapes, parameters, and arrangements of the nanoantennas can bring new applications and possibilities for nanoscale excitation and shaping of surface plasmons.

FUNDING INFORMATION

European Commission Marie Curie Career Integration (333821); Israeli Science Foundation (1331/13); Kamin (51387).

References

1. W. L. Barnes, A. Dereux, and T. W. Ebbesen, Nature **424**, 824 (2003).
2. E. Ozbay, Science **311**, 189 (2006).
3. J. S. Donner, G. Baffou, D. McCloskey, and R. Quidant, ACS Nano **5**, 5457 (2011).
4. H. A. Atwater and A. Polman, Nat. Mater. **9**, 205 (2010).
5. M. L. Brongersma and V. M. Shalaev, Science **328**, 440 (2010).
6. M. L. Juan, M. Righini, and R. Quidant, Nat. Photonics **5**, 349 (2011).
7. D. G. Grier, Nature **424**, 810 (2003).
8. S. A. Maier, M. D. Friedman, P. E. Barclay, and O. Painter, Appl. Phys. Lett. **86**, 071103 (2005).
9. S. I. Bozhevolnyi, V. S. Volkov, E. Devaux, J.-Y. Laluet, and T. W. Ebbesen, Nature **440**, 508 (2006).
10. P. Zhang, S. Wang, Y. Liu, X. Yin, C. Lu, Z. Chen, and X. Zhang, Opt. Lett. **36**, 3191 (2011).
11. C. J. Zapata-Rodrguez, S. Vuković, M. R. Belić, D. Pastor, and J. J. Miret, Opt. Express **19**, 19572 (2011).
12. A. Libster-Hershko, I. Epstein, and A. Arie, Phys. Rev. Lett. **113**, 123902 (2014).
13. I. Epstein and A. Arie, Phys. Rev. Lett. **112**, 023903 (2014).
14. I. Epstein and A. Arie, Opt. Lett. **39**, 3165 (2014).
15. I. Epstein, Y. Lilach, and A. Arie, J. Opt. Soc. Am. B **31**, 1642 (2014).
16. B. Hecht, H. Bielefeldt, L. Novotny, Y. Inouye, and D. Pohl, Phys. Rev. Lett. **77**, 1889 (1996).
17. M. V. Bashevoy, F. Jonsson, A. V. Krasavin, N. I. Zheludev, Y. Chen, and M. I. Stockman, Nano Lett. **6**, 1113 (2006).
18. E. Eizner and T. Ellenbogen, Appl. Phys. Lett. **104**, 223301 (2014).
19. P. E. Landreman and M. L. Brongersma, Nano Lett. **14**, 429 (2014).
20. P. Biagioni, J.-S. Huang, and B. Hecht, Rep. Prog. Phys. **75**, 024402 (2012).
21. V. Coello and S. Bozhevolnyi, Opt. Commun. **282**, 3032 (2009).
22. I. Smolyaninov, D. Mazzoni, J. Mait, and C. Davis, Phys. Rev. B **56**, 1601 (1997).
23. M. W. Knight, N. K. Grady, R. Bardhan, F. Hao, P. Nordlander, and N. J. Halas, Nano Lett. **7**, 2346 (2007).
24. D. Chang, A. S. Rensen, P. Hemmer, and M. Lukin, Phys. Rev. Lett. **97**, 053002 (2006).
25. L. Yin, V. K. Vlasko-Vlasov, J. Pearson, J. M. Hiller, J. Hua, U. Welp, D. E. Brown, and C. W. Kimball, Nano Lett. **5**, 1399 (2005).
26. O. Avayu, O. Eisenbach, R. Ditcovski, and T. Ellenbogen, Opt. Lett. **39**, 3892 (2014).
27. J. Lin, J. P. B. Mueller, Q. Wang, G. Yuan, N. Antoniou, X.-C. Yuan, and F. Capasso, Science **340**, 331 (2013).
28. N. Shitrit, I. Yulevich, E. Maguid, D. Ozeri, D. Veksler, V. Kleiner, and E. Hasman, Science **340**, 724 (2013).
29. N. Dahan, Y. Gorodetski, K. Frischwasser, V. Kleiner, and E. Hasman, Phys. Rev. Lett. **105**, 136402 (2010).
30. O. Keller, M. Xiao, and S. Bozhevolnyi, Surf. Sci. **280**, 217 (1993).
31. L. Froehly, F. Courvoisier, A. Mathis, M. Jacquot, L. Furfaro, R. Giust, P. A. Lacourt, and J. M. Dudley, Opt. Express **19**, 16455 (2011).
32. E. Greenfield, M. Segev, W. Walasik, and O. Raz, Phys. Rev. Lett. **106**, 213902 (2011).
33. D. McGloin, G. Spalding, H. Melville, W. Sibbett, and K. Dholakia, Opt. Commun. **225**, 215 (2003).